Interaction of the Membrane-Inserted Diphtheria Toxin T Domain with Peptides and Its Possible Implications for Chaperone-like T Domain Behavior†

Kelli Hammond,‡ Gregory A. Caputo,‡ and Erwin London*

Department of Biochemistry and Cell Biology and Department of Chemistry, State University of New York at Stony Brook, Stony Brook, New York 11794-5215

Received June 5, 2001; Revised Manuscript Received November 28, 2001

ABSTRACT: The T domain of diphtheria toxin is believed to aid the low-pH-triggered translocation of the partly unfolded A chain (C domain) through cell membranes. Recent experiments have suggested the possibility that the T domain aids translocation by acting as a membrane-inserted chaperone [Ren, J., et al. (1999) *Science 284*, 955−957]. One prediction of this model is that the membrane-inserted T domain should be able to interact with sequences that mimic unfolded proteins. To understand the basis of interaction of the membrane-inserted T domain with unfolded polypeptides, its interaction with water-soluble peptides having different sequences was studied. The membrane-inserted T domain was able to recognize helix-forming 23-residue Ala-rich peptides. In the presence of such peptides, hydrophobic helix 9 of the T domain underwent the previously characterized conformational change from a state exhibiting shallow membrane insertion to one exhibiting deep insertion. This conformational change was more readily induced by the more hydrophobic peptides that were tested. It did not occur at all in the presence a hydrophilic peptide in which alternating Ser and Gly replaced Ala or in the presence of unfolded hydrophilic peptides derived from the A chain of the toxin. Interestingly, a peptide with a complex sequence (RKE_3KE_2-$LMEW_2KM_2SETLNF$) also interacted with the T domain very strongly. We conclude that the membrane-inserted T domain cannot recognize every unfolded amino acid sequence. However, it does not exhibit strong sequence specificity, instead having the ability to recognize and interact with a variety of amino acid sequences having moderate hydrophobicity. This recognition was not strictly correlated with the strength of peptide binding to the lipid, suggesting that more than just hydrophobicity is involved. Although it does not prove that the T domain functions as a chaperone, T domain recognition of hydrophobic sequences is consistent with it having polypeptide recognition properties that are chaperone-like.

The process of protein translocation across lipid bilayers is poorly understood. Diphtheria toxin, a protein from *Corynebacterium diphtheriae*, is a useful model system for studying the translocation process. The crystal structure shows that this A−B toxin is composed of three domains: a catalytic (C) domain (residues 1−193), which is equivalent to its A chain, a transmembrane (T) domain (residues 194−381), and a receptor binding (R) domain (residues 382−535) (*1*). The latter two domains form the B chain. The R domain binds an EGF-related precursor protein (*2*). This association allows the toxin to undergo receptor-mediated endocytosis and enter endosomes. The acidic pH of the endosomal lumen causes a partial unfolding of the toxin, exposing hydrophobic regions on the T domain and thus triggering membrane insertion (*3*, *4*). This is followed by the translocation of the A chain into the cytosol, where it catalyzes the ADP ribosylation of elongation factor 2, and thus inhibits protein synthesis.

The mechanism by which the A chain is translocated across membranes remains mysterious after many years of study. At low pH, the A chain undergoes a reversible conformational change in which it partly unfolds and becomes hydrophobic (*5*, *6*). The unfolding of the A chain appears to be necessary for efficient translocation to occur (*7*−*9*). The membrane-inserted T domain is thought to assist in maneuvering the A chain through the membrane. Studies of the topography of the membrane-inserted toxin at low pH suggest that a state in which the A chain and part of the T domain have translocated across the membrane may be a (late?) intermediate in the translocation process (*7*, *10*, *11*). Detailed topography studies suggest everything N-terminal to T domain helix 5 may have translocated in this state (*11*). The pore formed by sequence elements within the T domain also appears to be connected with translocation in some fashion (*11*). However, because the A chain can interact with lipids at low pH (*5*, *6*, *12*), and because the size and role of the pore under physiological conditions are uncertain (*11*, *13*−*17*), it is not necessarily true that the A chain simply diffuses through an aqueous pore formed by the T domain (*3*).

We recently raised the possibility of a chaperone model for A chain translocation. According to this model, the hydrophobic and partly unfolded A chain passes through a "sticky" pore formed by the T domain via a number of relatively nonspecific and transient binding events. This model was proposed on the basis of the observation that the

† This work was supported by NIH Grant R01 GM31986.

* To whom correspondence should be addressed. Phone: (631) 632-8564. Fax: (631) 632-8575. E-mail: Erwin.London@sunysb.edu.

‡ These authors contributed equally to this work.

10.1021/bi011163i CCC: $22.00
Published on Web 02/02/2002

membrane-inserted T domain recognizes and binds to a number of different partly unfolded proteins believed to be in the molten globule state (*18*).

The increased hydrophobicity of proteins in the molten globule state might mean that the membrane-inserted T chain recognizes somewhat hydrophobic sequences. Alternately, it might be able to recognize any unfolded amino acid sequence, whether in the molten globule state or random coil state, and interactions other than hydrophobicity (e.g., hydrogen bonding) might be involved. In this report, the sequence requirements for polypeptide interaction with the membrane-inserted T domain have been probed by examining T domain interaction with various peptides. The results suggest hydrophobicity is one important factor in sequence recognition by the T domain, although the details of peptide sequence modulate this interaction.

EXPERIMENTAL PROCEDURES

Materials. Dioleoyl-*sn*-glycero-3-phosphocholine (DOPC),[1] dimyristoleoyl-*sn*-glycero-3-phosphocholine (DMoPC), dioleoyl-*sn*-glycero-3-phosphoglycerol (DOPG), 1-palmitoyl-2-(12-doxyl)stearoyl-*sn*-glycero-3-phosphocholine (12SLPC), 1-palmitoyl-2-oleoyl-*sn*-glycero-3-phosphotempocholine (TempoPC), and lissamine rhodamine B-labeled dipalmitoyl-*sn*-glycero-3-phosphoethanolamine (rhodamine-PE) were purchased from Avanti Polar Lipids (Alabaster, AL). Lipid concentrations were determined by dry weight. The fluorescent probe 6-(bromoacetyl)-2-(dimethylamino)naphthalene (badan) was purchased from Molecular Probes (Eugene, OR).

Acetyl-$K_2A_9WA_9K_2$-amide (A18 peptide), acetyl-$K_2LA_8WA_8LK_2$-amide (A16L2 peptide), acetyl-$K_2LA_7LWLA_7LK_2$-amide (A14L4 peptide), acetyl-$K_2L(SG)_4W(SG)_4LK_2$-amide [(SG)8L2 peptide], acetyl-$K_2GL_9WL_9K_2$A-amide, acetyl-K_2-$CWL_9AL_9K_2$A-amide, TRGKRGQDAMYEYMAQA (A chain residues 168−184), KAGGVVKVTYPGLTKVLALKV (A chain residues 76−96), and FIKRFGDGASRVVLSLPFA (A chain residues 123−141) were purchased from Research Genetics (Huntsville, AL). The (SG)8L2 peptide was used without purification except in the CD experiments. In all other cases, the peptides were purified by HPLC, and purity was assayed by mass spectrometry as described previously (*19*, *20*). For the Ala-rich, (SG)8L2, and A chain peptides, the purification procedure was altered slightly as follows. These peptides were dissolved in water, and eluted with a shallow gradient starting with water containing 0.5% (v/v) trifluoroacetic acid (TFA) and then increasing amounts of 2-propanol containing 0.5% TFA. Fractions containing purified peptides were dried and then dissolved at a concentration of ~0.2−0.3 mM in 10 mM Tris-HCl and 150 mM NaCl (pH 8.0). (When necessary, the pH was readjusted to 8.0 after buffer was added to the peptide.) The peptides were stored at 4 °C. CP peptide, which has a sequence from the C-terminus of carboxypeptidase E, $RKE_3KE_2LMEW_2$-$KM_2SETLNF$, was a gift from Y. Peng Loh (National Institutes of Health, Bethesda, MD). It was found to be pure by MALDI-TOF mass spectrometry. The CP peptide was dissolved in 10 mM Tris-HCl and 150 mM NaCl (pH 8.0) at a concentration of 0.3−0.8 mM and stored at 4 °C.

T Domain Purification. The diphtheria toxin T domain with single Cys substitutions was isolated from *Escherichia coli* transformed with a T domain-carrying plasmid using a protocol similar to that described previously (*21*). Three different His-tagged T domain mutants (H322C, E349C, and A356C) and the "wild-type" T domain (encompassing diphtheria toxin residues 202−378) were used (*21*, *24*). After expression of the T domain, it was released from cells by treatment with lysozyme and sonication (*21*). The supernatant produced after centrifugation (to remove cell debris) was chromatographed on a (Talon) cobalt-containing affinity resin (Clontech, Palo Alto, CA). Generally, a column containing ~1.5 mL of resin was washed with 1 mL of 0.25× wash buffer [1× wash buffer was 90 mM imidazole, 0.5 M NaCl, and 20 mM Tris-HCl (pH 8)], then 1 mL of 0.5× wash buffer, 1 mL of 0.75× wash buffer, 1 mL of 1× wash buffer, and finally a series of individual 0.5 mL aliquots of elution buffer [1 M imidazole, 0.5 M NaCl, and 20 mM Tris-HCl (pH 8)]. The T domain tended to elute in the last wash buffer and first two aliquots of elution buffer. The T domain fractions were combined, diluted to 50 mL with 20 mM Tris-HCl (pH 8), and then subjected to FPLC on a 1 mL Source-Q anion exchange column (Pharmacia Biotech, Piscataway, NJ), eluting at a rate of 0.5 mL/min with a 0 to 500 mM NaCl gradient containing 20 mM Tris-HCl (pH 8). The T domain eluted at ~250 mM NaCl. The purified fractions (as detected by SDS gel electrophoresis) were combined and stored at 4 °C. The final protein concentration was between 0.3 and 2 mg/mL. The His tag at the N-terminus was not removed (*21*). Generally, the final purity appeared to be >95% as judged by SDS gel electrophoresis. The T domain concentration was determined from the absorbance at 280 nm using an ϵ of 18 200 M^{-1} cm^{-1}, and converted to micrograms using an approximate molecular weight of 20 000. The intact hexahistidine-tagged A chain was expressed and purified using similar techniques (M. Hayashibara and E. London, unpublished observations). The construct that was used consisted of A chain residues 1−189, with an N-terminal hexahistidine tag, a Cys at residue 1 replacing that at residue 186, and the E148S substitution, which abolishes toxicity. This protein behaved like the wild-type A chain (not shown).

Fluorescence Labeling of the T Domain. The T domain was labeled with badan using a procedure similar to that used previously for BODIPY and bimane labeling (*21*). For labeling, 6 μL of 8 mM badan dissolved in ethanol was added to a 100 μg sample of the T domain diluted to 1 mL with 10 mM Tris-HCl and 150 mM NaCl (pH 8) (giving a badan:T domain molar ratio of ~10:1). The sample was then incubated with mixing at room temperature for 15 min. The reaction was quenched with dithiothreitol in water (10 mM final concentration). The sample was then dialyzed overnight (using 8000 MW cutoff tubing) against 5 L of 10 mM Tris-HCl (pH ~8) and stored at 4 °C. As a control, the labeling of the wild-type T domain, which lacks Cys, was performed in parallel during every labeling experiment. The badan

[1] Abbreviations: A18 peptide, acetyl-$K_2A_9WA_9K_2$-amide; A16L2 peptide, acetyl-$K_2LA_8WA_8LK_2$-amide; A14L4 peptide, acetyl-K_2LA_7-$LWLA_7LK_2$-amide; badan, 6-(bromoacetyl)-2-(dimethylamino)naphthalene; CP peptide, $RKE_3KE_2LMEW_2KM_2SETLNF$; DMoPC, dimyristoleoyl-*sn*-glycero-3-phosphocholine; DOPC, dioleoyl-*sn*-glycero-3-phosphocholine; DOPG, dioleoyl-*sn*-glycero-3-phosphoglycerol; rhodamine-PE, lissamine rhodamine B dipalmitoyl-*sn*-glycero-3-phosphoethanolamine; (SG)8L2 peptide, acetyl-$K_2L(SG)_4W(SG)_4LK_2$-amide; 12SLPC, 1-palmitoyl-2-(12-doxyl)stearoyl-*sn*-glycero-3-phosphocholine; SUV, small unilamellar vesicles; TempoPC, 1-palmitoyl-2-oleoyl-*sn*-glycero-3-phosphocholine.

fluorescence was always at least 10-fold higher in the Cys-containing mutants than in the wild type.

Fluorescence Measurements. Fluorescence was measured at room temperature with a Spex Tau 2 Fluorolog spectrofluorometer operating in steady state mode. Unless otherwise noted, measurements were made in a semi-micro quartz cuvette (excitation path length of 10 mm, emission path length of 4 mm). The excitation and emission slit widths were 1.5 mm (2.5 mm for acrylamide experiments) and 5 mm, respectively. Trp emission spectra were measured at a rate of 1 nm/s using excitation at 280 nm. Badan emission spectra were measured at a rate of 1 nm/s with excitation at 375 nm.

Preparation of Model Membranes and Incorporation of the T Domain. Small unilamellar vesicles (SUV) were prepared from mixtures containing 2.5 μmol of total lipid composed of 80% DOPC and 20% DOPG, 80% DMoPC and 20% DOPG, 10% TempoPC, 70% DOPC, 20% DOPG, or 30% 12SLPC, 50% DOPC, and 20% DOPG (molar ratios). The lipid mixtures, prepared from solutions in $CHCl_3$ or ethanol, were dried under a stream of N_2 at ~30 °C, redissolved in a few drops of $CHCl_3$, redried with N_2, and then further dried under high vacuum for 30 min. Samples were then hydrated with 500 μL of Tris-acetate buffer [6.7 mM Tris-HCl, 150 mM NaCl, and 167 mM sodium acetate (pH 4.1)] and sonicated in a bath sonicator (model G112SP1T, Lab Supplies Co., Hicksville, NY) for 25 min or until they were optically clear.

Typically, to incorporate the T domain into model membranes, a 26 μL aliquot of sonicated vesicles (5 mM lipid) was mixed with 614 μL of Tris-acetate (pH 4.1). Then 10 μL (containing 1 μg of protein) of the badan-labeled T domain mutant was added, and mixed with a micro-stir bar for ~2 min.

Fluorescence Emission of the Badan-Labeled T Domain versus Peptide Concentration. Samples of the membrane-incorporated T domain were prepared as described above. Small aliquots (2−15 μL) of the peptide (from stock solutions of approximately 200−300 μM) were then added and then mixed with a micro-stir bar. The small amount of buffer in the peptide did not affect the sample pH. After ~30 s of mixing, badan fluorescence emission was measured. There was an incubation time of at least 1 min between the additions of each aliquot. This was sufficient for peptide-induced shifts in badan fluorescence to reach final values (not shown). The ratio of emission at 502 nm to that at 470 nm was calculated after subtracting the intensity of background intensity from controls lacking protein.

Assessment of Peptide Binding to Lipid Vesicles. Samples containing 2 or 10 μM peptide were prepared by mixing 15−35 μL of a 200−300 μM stock peptide with Tris-acetate buffer (pH 4.1) to give a volume of 650 μL. After a tryptophan fluorescence emission spectrum had been recorded, samples were titrated with 3−10 μL aliquots of SUV (5 mM lipid) as described above. Trp fluorescence emission spectra were measured after each addition. Lipid-induced shifts in peptide fluorescence reached final values immediately after each addition (not shown). Background intensity (from samples lacking peptide) was found to be negligible. The results reported for 10 μM peptide are the average of duplicate experiments.

Peptide binding to lipid vesicles was also assayed by fluorescence quenching. To do this, peptides were titrated in a manner similar to that described above, using both 80% DOPC/20% DOPG SUV and either 30% 12SLPC/50% DOPC/20% DOPG SUV (molar ratio) or 10% TempoPC/70% DOPC/20% DOPG SUV (molar ratio). At each lipid concentration, the fluorescence intensity in these samples was measured at the λ_{max} of Trp emission in the absence of lipid (356−360 nm on our instrument), and then the values that were obtained were corrected for background fluorescence. The corrected intensity values in samples containing SUV with quencher (12SLPC) were divided by the corresponding values in samples containing SUV without quencher, to yield F/F_o, the fraction of unquenched fluorescence.

λ_{max} of Different Badan-Labeled T Domain Residues in the Absence and Presence of Peptides. Samples of the membrane-incorporated T domain were prepared by diluting 26 μL of SUV (from a 5 mM lipid stock composed of 80% DOPC/20% DOPG SUV or 80% DMoPC/20% DOPG SUV) with 614 μL of Tris-acetate buffer (pH 4.1). Then 10 μL of 100 μg/mL badan-labeled T domain (H322C, E349C, or A356C mutant) was added while stirring with a micro-stir bar. For each sample, a badan fluorescence emission spectrum was measured as described above, and then CP peptide or A14L4 peptide was added to a concentration of 25 μM (usually between 50 and 80 μL from a 200−300 μM stock peptide). The pH remained 4.1. The badan fluorescence spectrum was then remeasured. Background spectra from samples lacking protein were also collected and subtracted from the sample spectra before the badan λ_{max} was calculated.

Column Chromatography of Peptide/T Domain/SUV Mixtures. Samples containing a mixture of SUV, T domain, and peptide were prepared. Each contained 1 mM SUV (80% DOPC/20% DOPG) with a trace amount of rhodamine-PE, 7.5 μg/mL badan-labeled T(A356C) domain, and 50 μM A16L2 peptide, or 6 μM CP peptide, or no peptide. Samples were diluted to a final total volume of 1 mL with Tris-acetate (pH 4.1) and then subjected to size chromatography on a Sepharose CL-4B (Pharmacia Biotech) gel filtration column (30 cm length × 1 cm diameter). Fractions of approximately 600 μL were collected. In each fraction, the fluorescence of Trp (excitation at 280 nm, emission at 330 nm), badan (excitation at 375 nm, emission at both 470 and 502 nm), and rhodamine (excitation at 565 nm, emission at 585 nm) was measured to follow the elution profiles for the peptide, T domain, and lipid, respectively. (In the presence of the peptide, the contribution of the T domain to Trp fluorescence could be ignored.) The total recovery of lipid in the fractions was roughly 66−75%. The recovery of peptide was roughly 40% for the CP peptide and 75% for the A16L2 peptide. The recovery of the T domain (based on badan fluorescence) was on the order of $^1/_3$ to $^1/_5$ of that of the lipid. We do not know if this was due to bleaching of the badan group, or loss of protein on the column. T domain recovery was similar in the absence of presence of peptides.

Acrylamide Quenching Experiments. For samples containing A14L4 peptide, an aliquot of SUV composed of 80% DOPC and 20% DOPG (molar ratio) was mixed with peptide and Tris-acetate (pH 4.1) to yield concentrations of 200 μM or 1 mM lipid and 10 μM peptide in a volume of 800 μL. For the transmembrane peptides (acetyl-$K_2GL_9WL_9K_2A$-amide and acetyl-$K_2CWL_9AL_9K_2A$-amide), acrylamide

quenching was assessed in 200 μM DOPC vesicles prepared by ethanol dilution into 10 mM phosphate and 150 mM NaCl (pH 7.1) as previously described (*20*, *21*). In all cases, aliquots of acrylamide were added from a 4 M stock solution dissolved in water. Approximately 2−3 min after each aliquot was added, the Trp fluorescence was measured at an excitation wavelength of 295 nm and an emission wavelength of 340 nm. Addition of acrylamide did not affect the pH. Background intensity values from samples lacking peptide were subtracted from the values in the presence of peptide, and the resulting fluorescence intensities were corrected both for dilution and for the inner filter effect arising from acrylamide absorbance (*22*). The ratio of fluorescence intensity in the absence of acrylamide to that in its presence (F_o/F) was then calculated.

Measurement of Circular Dichroism. Circular dichroism (CD) measurements were taken in 1 mm path length quartz cuvettes at room temperature using a Jasco J-715 CD instrument. Samples without lipid contained an aliquot of peptide (to give a final concentration of 5 μM) diluted to 650 μL with Tris-acetate (pH 4.1) that had been diluted 10-fold with water (the final pH remained 4.1). Samples with 5 μM peptide were also prepared mixed with 80% DOPC/20% DOPG (molar ratio) sonicated SUV, and then diluted to 650 μL in 0.1× Tris-acetate (pH 4.1). The final lipid concentration was 200 μM. Approximately 100−150 spectra were collected and averaged for each measurement. Background values from samples lacking peptide were subtracted, and after conversion to molar ellipticity (per peptide bond), the α-helix fraction was calculated using SELCON3 (*23*).

RESULTS

Detecting Conformational Changes in the Membrane-Bound T Domain with Fluorescence. The T domain spontaneously inserts into model membrane vesicles at low pH. Fluorescently labeling residues in hydrophobic helices 8 and 9 of the T domain allows detailed evaluation of environment of these helices in the membrane-inserted state (*21*, *24*). Previous studies have shown that there is a conformation change that can occur in the membrane-inserted T domain in which helices 8 and 9 move from a surface location to a deeply inserted (and apparently transmembraneous) state (*24*). This change can be detected by a characteristic blue shift of bimane emission in the deeply inserted state (*21*, *24*). The fluorescence of the T domain labeled on a Cys introduced at residue 356 (A356C), which is within the core of helix 9, is particularly sensitive to this conformational change (*21*).

To further increase the response of fluorescence to this conformational change, we labeled residue 356 with badan which, like the closely related prodan and acrylodan probes (*25*), has a fluorescence emission spectrum that is especially sensitive to environment. The behavior of the badan-labeled T domain was compared to that of the bimane-labeled T domain to confirm that badan fluorescence responds in the same manner as that of bimane. To do this, T domain mutants with badan-labeled single Cys residues at position 356, 322, or 349 were used. (Residues 322 and 349 are just outside of the hydrophobic segments of helices 8 and 9.) Table 1 shows that under conditions in which helices 8 and 9 of the membrane-inserted T domain are located along the membrane surface [i.e., in 4:1 DOPC/DOPG SUV (*21*, *24*)] badan-labeled residues 322, 349, and 356 all exhibit red-shifted fluorescence (monitored by the ratio of fluorescence at 502 nm relative to that at 470 nm[2]). This is the expected result for shallow insertion, and is behavior similar to that observed in previous studies with the bimane-labeled T domain (*21*, *24*).

Table 1: Comparison of Shifts in Badan Spectra of the Model Membrane-Inserted T Domain Labeled with Badan at Residue 322, 349, or 356[a]

	F_{502}/F_{470}		
sample	residue 322	residue 349	residue 356
T in 4:1 DOPC/DOPG SUV (shallowly inserted)	0.96	1.03	0.97
T in 4:1 DMoPC/DOPG SUV (deeply inserted)	0.96	1.06	0.67
T in 4:1 DOPC/DOPG SUV with CP peptide	0.95	1.00	0.70
T in 4:1 DOPC/DOPG SUV with A14L4 peptide	0.87	0.85	0.67

[a] These values were calculated from the average of two experiments. For samples containing the T domain inserted into DOPC/DOPG vesicles, fluorescence intensity was measured before and after peptide addition. The range of F_{502}/F_{470} values was ±0.03 for residues 322 and 349 and up to ±0.1 for residue 356. However, the change in F_{502}/F_{470} upon addition of peptide to the T domain inserted into DOPC/DOPG vesicles was reproducible to ±0.02 in all cases.

In 4:1 DMoPC/DOPG SUV, helices 8 and 9 take on the deeply inserted conformation (*21*), and bimane-labeled residue 356 exhibits a marked blue shift of fluorescence relative to that in the surface conformation (*21*). However, bimane-labeled residues 322 and 349 remain in the polar environment outside of the bilayer core in the deeply inserted state, and fail to exhibit a strong blue shift (*21*, *24*). Table 1 shows the same pattern holds for the T domain with badan-labeled residues 322, 349, and 356 that are inserted into 4:1 DMoPC/DOPC SUV.

Interaction of Peptides with the T Domain. We previously used the change of the T domain from the shallowly inserted state to the deeply inserted state, monitored by fluorescent labels attached to residue 356, to detect binding of proteins to the model membrane-inserted T domain (*18*, *21*). A similar approach was taken to examine peptide interaction with the model membrane-inserted T domain. The first peptides that were chosen were a series of moderately hydrophobic, but water soluble, peptides with an Ala-rich sequence ($K_2A_9WA_9K_2$, $K_2LA_8WA_8LK_2$, and $K_2LA_7LWLA_7LK_2$, named the A18 peptide, the A16L2 peptide, and the A14L4 peptide, respectively), and one hydrophilic peptide in which a Ser-Gly repeat replaces Ala [$K_2L(SG)_4W(SG)_4LK_2$, named the (SG)8L2 peptide]. The Trp residue in the center of these sequences allows spectroscopic evaluation of their behavior. We also used a peptide with a complex sequence derived from a membrane-associating segment of carboxypeptidase E ($RKE_3KE_2LMEW_2KM_2SETLNF$, named the CP peptide) (*26*).

[2] The ratio of fluorescence at two wavelengths was used to monitor shifts in badan fluorescence emission rather than emission λ_{max}. Badan λ_{max} is very different in polar and nonpolar environments, and instead of a representative average λ_{max}, mixtures of blue- and red-shifted badan molecules tend to give partially resolved peaks in which the less abundant form appears as a shoulder on the spectrum of the more abundant form.

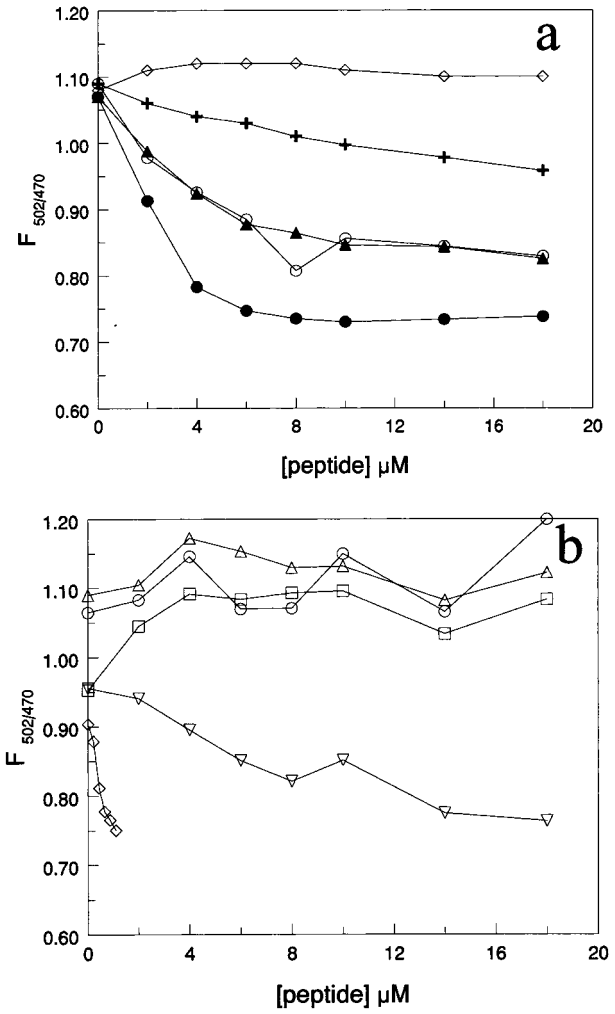

FIGURE 1: Effect of peptides on the badan fluorescence of the model membrane-inserted T domain. Samples contained 1.5 μg/mL badan-labeled A356C T domain bound to 200 μM SUV composed of a 4:1 (molar ratio) DOPC/DOPG mixture in Tris-acetate (pH 4.1). (a) Small aliquots of (◇) (SG)8L2 peptide, (+) A18 peptide, (○) A16L2 peptide, (▲) A14L4 peptide, or (●) CP peptide were then added. The results of one experiment are shown, but similar results were obtained in two other experiments. (b) Small aliquots of (◇) intact A chain, (▽) A14L4 peptide, (○) A chain residues 76−96, (△) A chain residues 123−141, or (□) A chain residues 168−184 were added. The average of two values is shown. Individual values were generally within ±0.05 of the average value. The *y*-axis is the ratio of badan fluorescence emission intensity at 502 nm to that at 470 nm.

To examine the effects of these peptides on the T domain, they were added to samples containing the T domain that was shallowly membrane-inserted, as shown by the characteristically red-shifted fluorescence of badan-labeled residue 356. Figure 1a and Table 2 show that under these conditions most peptides induce a strong blue shift in badan fluorescence, indicating they induce conversion of the T domain into a more deeply inserted conformation. The degree of blue shift depends on peptide sequence, with a decreasing shift in the following order: CP peptide > A14L4 peptide = A16L2 peptide > A18 peptide > (SG)8L2 peptide. It is noteworthy that in general the more hydrophobic peptides interact with the T domain more strongly. Addition of the relatively hydrophilic (SG)8L2 peptide does not cause any blue shift in badan fluorescence.

Table 2: Effects of Peptides on the Fluorescence of the Model Membrane-Inserted T Domain Labeled with Badan at Residue 356[a]

	$\Delta F_{502}/F_{470}$ for badan	
peptide	4 μM peptide	10 μM peptide
(SG)8L2	<0.01	<0.01
A18	0.09 ± 0.08	0.12 ± 0.06
A16L2	0.21 ± 0.06	0.28 ± 0.06
A14L4	0.22 ± 0.05	0.30 ± 0.08
CP	0.37 ± 0.07	0.38 ± 0.04

[a] $\Delta F_{502}/F_{470}$ equals F_{502}/F_{470} in the absence of peptide minus F_{502}/F_{470} in the presence of peptide. Except for the (SG)8L2 peptide, for which two experiments were performed, the average values and the standard deviations for three experiments are shown.

The effect of the A14L4 and CP peptides on the T domain conformation was further examined by comparing their effects on the membrane-inserted T domain with badan-labeled residue 322 or 349 to their effects on the membrane-inserted T domain with badan-labeled residue 356. As shown in Table 1, in contrast to the strong blue shift induced when residue 356 is labeled with badan, the CP peptide does not induce any significant blue shift in residue 322 or 349. This pattern is almost identical to that observed under other conditions in which the deeply inserted conformation forms, e.g., when the T domain inserts into 4:1 DMoPC/DOPG vesicles (*21*, *24*). The lack of deep insertion by residues 322 and 349 when helices 8 and 9 insert deeply is expected because they are in the hydrophilic sequences flanking these helices.

In contrast to the behavior upon addition of the CP peptide, addition of the A14L4 peptide does induce a significant blue shift of the fluorescence of badan-labeled residue 349, and a weak blue shift in badan-labeled residue 322. However, both shifts are much smaller than the shift the peptide induces in badan-labeled residue 356. This suggests that the conformational change induced in the membrane-inserted T domain by the A14L4 peptide is similar, but not identical, to that induced by the CP peptide and other conditions that result in deep, transmembraneous insertion (*21*, *24*).

We then examined the interaction of the T domain with the intact A chain, and with three peptides corresponding to sequences within the A chain. In the native, intact A chain, two of the peptides that were studied (with sequences identical to A chain residues 76−96 and 123−141) overlap with β-strands that have the potential ability to form transmembrane segments, i.e., forming strands that have alternating sequences of hydrophobic and hydrophilic residues (*7*). The third (A chain residues 168−184) corresponds to the C-terminal part of the A chain, which has been proposed to be the part of the A chain that translocates first (*9*).

As shown in Figure 1b, none of the A chain peptides is able to induce a blue shift in badan fluorescence. This contrasts with the strong blue shift observed with the intact A chain. In fact, the intact A chain is able to induce a blue shift at a concentration almost 1 order of magnitude lower than that of any of the peptides that were tested.

Peptide Properties and Lipid Interaction. We were interested in understanding how the physical properties of peptides might be related to their interaction, or lack of interaction, with the T domain. For example, the observation that for the Ala-rich peptides the effect on the T domain

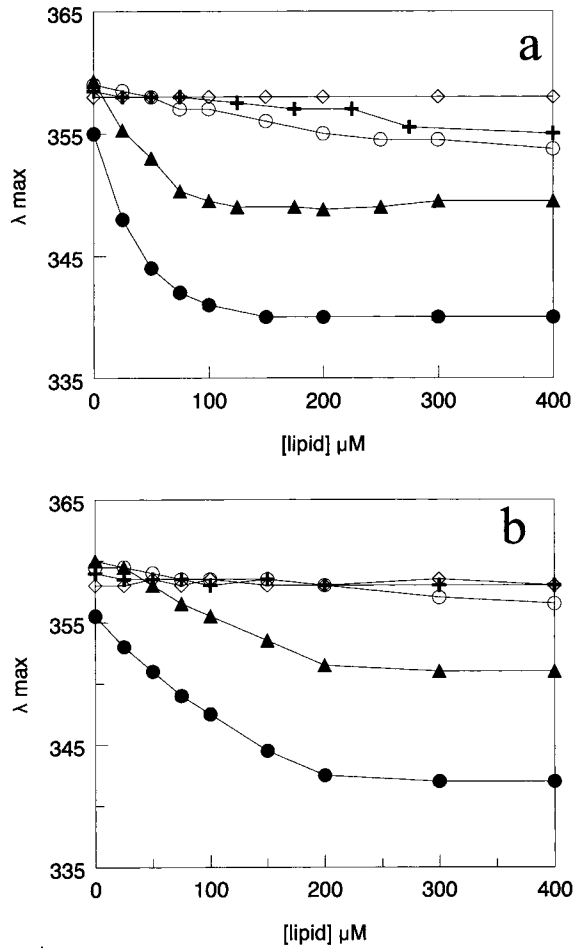

FIGURE 2: Binding of peptides to lipid bilayers monitored through changes in tryptophan fluorescence emission wavelengths. The dependence of Trp emission λ_{max} on lipid concentration is shown for samples containing (a) 2 or (b) 10 μM peptide to which aliquots of 4:1 (molar ratio) DOPC/DOPG SUV in Tris-acetate (pH 4.1) were added. The final pH was 4.1. λ_{max} values were reproducible to $\pm$1 nm.

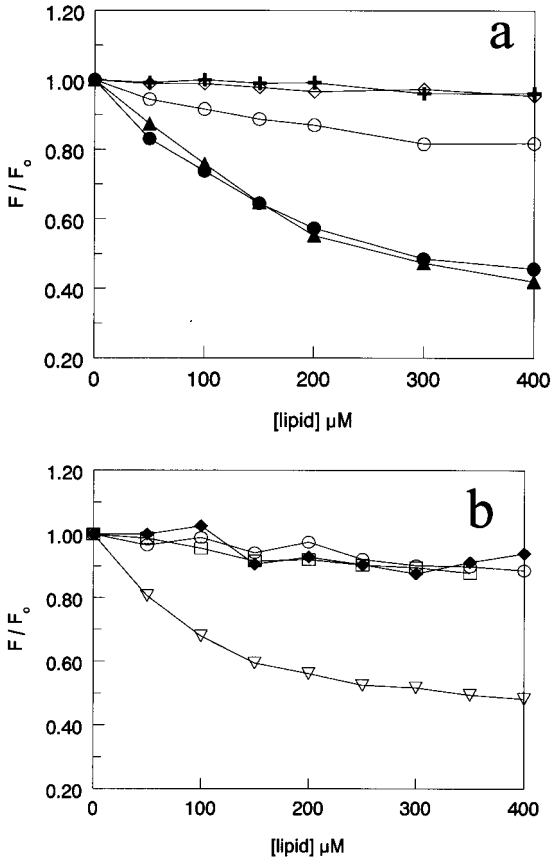

FIGURE 3: Dependence of Trp quenching by nitroxide-labeled lipid on lipid concentration. Samples contained 10 μM peptide to which aliquots of 4:1 (molar ratio) DOPC:DOPG SUV or (a) 5:3:2 (molar ratio) DOPC/12SLPC/DOPG SUV or (b) 7:2:1 (molar ratio) DOPC/DOPG/TempoPC SUV in Tris-acetate (pH 4.1) were added. F/F_o is the ratio of fluorescence in the samples containing vesicles containing quencher (12SLPC or TempoPC) to that in samples containing vesicles lacking quencher: (a) (◇) (SG)8L2 peptide, (+) A18 peptide, (○) A16L2 peptide, (▲) A14L4 peptide, and (●) CP peptide and (b) (◆) (SG)8L2 peptide, (▽) A14L4 peptide, (○) A chain residues 76−96, and (□) A chain residues 168−184.

was linked to peptide hydrophobicity could mean that there is a binding site(s) on the T domain that associates with hydrophobic peptides more effectively than hydrophilic ones. Alternately, it is conceivable that increased peptide hydrophobicity is important simply because it results in increased peptide binding to vesicles, which in turn would result in increased peptide binding to the T domain due to the resulting high local peptide concentration adjacent to the protein.

To distinguish between these possibilities, the binding of the different peptides to 4:1 DOPC/DOPG SUV was compared. Binding was assessed via shifts in the λ_{max} of the Trp in the sequence of each peptide that contained a Trp. A significant blue shift in Trp fluorescence is commonly observed when a Trp-containing peptide moves from an aqueous solution to a membrane-bound state. Panels a and b of Figure 2 show the dependence of peptide Trp λ_{max} on lipid concentration. There is no shift observed with the (SG)-8L2 peptide upon addition of lipid vesicles, suggesting it does not interact with the vesicles significantly. In contrast, the CP and A14L4 peptides exhibit a strong wavelength shift in the presence of lipid. The midpoint of the shift, which roughly speaking is the point at which peptide binding to lipid is half-maximal,[3] is equal for these peptides. The A18 and A16L2 peptides give very weak shifts, suggesting binding to vesicles that is much weaker than that of the CP and A14L4 peptides.[4]

To confirm these results, and extend them to the A chain peptides (which lack Trp), peptide binding to vesicles was also assessed by the quenching of peptide Trp or Tyr fluorescence by nitroxide-labeled lipids incorporated into the lipid bilayer (*27*). As shown in Figure 3a, for the Ala-rich peptides, quenching of 10 μM peptide in the presence of 4:1 PC/PG vesicles in which the nitroxide-labeled lipid 12SLPC was incorporated follows the same pattern as the

[3] There was little change in the overall Trp fluorescence intensity (<20% at λ_{max}) upon peptide binding to vesicles (not shown). For that reason, and because the overall shift in emission wavelength is small, the shift in Trp λ_{max} should be roughly proportional to the level of binding.

[4] The apparently weaker binding to lipid at 10 μM peptide relative to 2 μM peptide is curious. One possibility is that there is a peptide oligomerization and/or aggregation in solution that competes with lipid binding, especially at the higher peptide concentrations. Another is a limited number of binding sites per vesicle. This could be the case if the small amount of exposed hydrophobic surface in highly curved SUV forms the binding site for peptides. Consistent with this idea, the CP peptide was found to be unable to bind to large unilamellar vesicles, which lack such curvature (data not shown).

λ_{max} shifts. Figure 3b shows that this was not due to the position of the quencher on the lipid, as quenching of the (SG)8L2 and A14L4 peptides in the presence of analogous vesicles containing a lipid with a shallower quencher group, TempoPC, was similar to that with 12SLPC. Figure 3b also shows that Tyr residues on two of the A chain peptides (A chain residues 76−96 and 168−184) are unquenched in vesicles containing TempoPC, showing these peptides do not bind to these vesicles. [The binding to lipid of the A chain peptide of residues 123−141, which lacks Trp and Tyr, could not be examined by either λ_{max} or quenching. However, the response of its secondary structure to the presence of lipid indicates it does bind lipid to some degree (see below).]

A comparison of Figures 1−3 indicates that the effect of peptides on the T domain conformation does not fully correlate with their binding to lipid. In particular, the A16L2 and A14L4 peptides have an approximately equal effect on T domain fluorescence, despite stronger binding to lipid by the latter peptide. In addition, there is some effect on T domain conformation by A18 peptide, which binds to lipid very weakly, whereas the A chain peptide of residues 123−141 had no effect on T domain conformation despite some ability to bind to lipid. Thus, it is likely that at least some of the specificity of T domain−peptide interactions for hydrophobic peptides comes from the T domain, and that binding is not solely a nonspecific consequence of peptide binding to lipid.

Additional peptide properties that might provide insights into peptide−T domain interaction were also examined. λ_{max} can be used to estimate the position of the Trp-containing peptides within the bilayer. To do this, the emission wavelengths of membrane-bound CP and A14L4 peptides were compared to the standard curve of Trp λ_{max} versus depth we reported previously (*20*). The fluorescence of the CP and A14L4 peptides is even more red-shifted than that for a Trp at the polar−nonpolar boundary of the bilayer [for which λ_{max} is 338 nm (*20*)]. This strongly suggests that both the CP and A14L4 peptides are shallowly inserted. (We believe the other peptides also insert shallowly. However, their weak binding to lipid or lack of Trp precluded the use of λ_{max} measurements to estimate their depth.)

Acrylamide quenching was used to confirm that CP and A14L4 peptides occupy very shallow locations in the bilayer. Fluorescence quenching of Trp by acrylamide is dependent on the degree of Trp exposure to the aqueous environment (*29*). Previous studies show that the level of exposure of Trp to acrylamide decreases with increasing Trp depth in a bilayer (*29*, *30*). As shown in Figure 4, the difference between acrylamide quenching (as judged by K_{sv}, the slope of the F_o/F vs [acrylamide] curve) when a Trp is at the center of the bilayer and when it is at the polar−nonpolar boundary is marked.[5] Figure 4 shows the level of acrylamide quenching of the Trp of A14L4 is greater than that of a Trp at the polar−nonpolar boundary, confirming a shallow Trp location. Similar results were obtained with the CP peptide (*26*). Again, binding of the other peptides was too weak to allow assessment of acrylamide quenching of fully lipid-bound peptides. That the quenching of the A14L4 peptide at 200 μM lipid is not affected by a small amount of unbound peptide is confirmed by the observation that acrylamide quenching was similar when the lipid concentration was increased to 1 mM (Figure 4). This additional lipid should bind any residual peptide remaining dissolved in solution at 200 μM lipid.

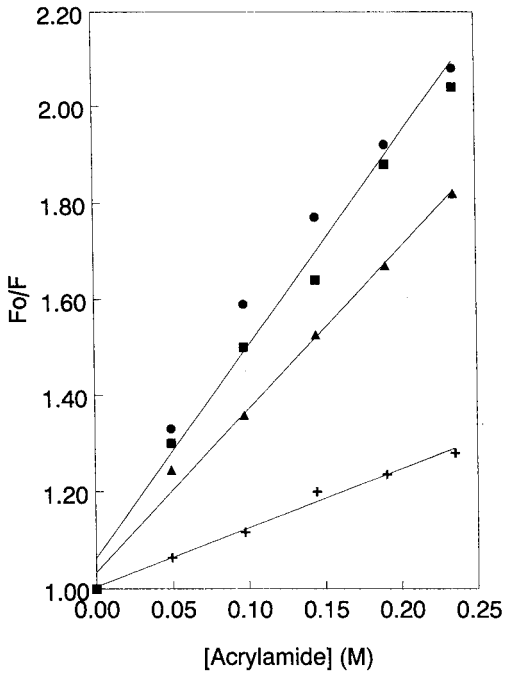

FIGURE 4: Acrylamide quenching of model membrane-incorporated peptides. Aliquots of acrylamide were added to samples containing 10 μM peptide incorporated into SUV. F is the fluorescence in the presence of acrylamide. F_o is the fluorescence in the absence of acrylamide: (+) acetyl-$K_2GL_9WL_9K_2A$-amide in 200 μM DOPC vesicles (pH 7.1), (▲) acetyl-$K_2CWL_9AL_9K_2A$-amide in 200 μM DOPC vesicles (pH 7.1), (●) A14L4 peptide in 200 μM 4:1 (molar ratio) DOPC/DOPG vesicles, and (■) A14L4 peptide in 1 mM 4:1 (molar ratio) DOPC/DOPG vesicles (pH 4.1). Acrylamide concentrations on both sides of the bilayer should be equal as acrylamide rapidly translocates through lipid bilayers (not shown). The average of duplicate samples, which differed by a few percent at most, is shown.

We also examined the secondary structure of the peptides (Figure 5). CD spectra of the (SG)8L2 peptide indicate it has a largely unordered structure in solution (Figure 5a). It was unaffected by the presence of lipid. In contrast, the Ala-rich peptides all exhibit CD spectra characteristic of a partially helical structure in solution. The signal increases to values characteristic of predominantly helical structures in the presence of lipid (Figure 5b).

The secondary structure of the A chain peptides is shown in Figure 6. An A chain peptide of residues 123−141 behaves like the Ala-rich peptides, in both the absence and presence of lipid (compare panels a and b of Figure 6). In contrast, A chain peptides of residues 76−96 and 168−184 exhibit a CD signal characteristic of a predominantly random structure both in solution and in the presence of bilayers. The lack of an effect of lipid on the CD spectra of these two peptides is not surprising given their inability to bind to lipid to a significant degree. It should be noted that the secondary structures of the A chain peptides are different from those they exhibit when part of the native toxin at neutral pH (*1*). However, what structure these sequences form in membrane-inserted toxin is unknown.

[5] This does not distinguish between the effects of depth on exposure to acrylamide and effects of depth on Trp fluorescence lifetime, as K_{sv} is proportional to both.

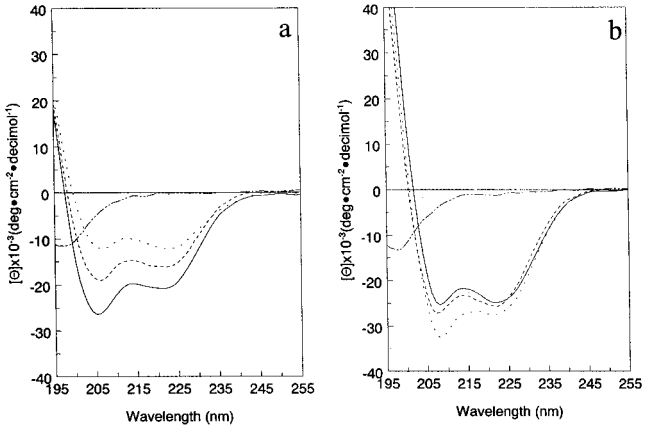

FIGURE 5: Circular dichroism spectra of model membrane-incorporated peptides. Samples contained 5 μM peptide in (a) 10-fold diluted Tris-acetate (pH 4.1) or (b) 10-fold diluted Tris-acetate (pH 4.1) with 200 μM 4:1 DOPC/DOPG SUV: (— - - —) (SG)-8L2 peptide, (- - -) A18 peptide, (—) A16L2 peptide, and (· · ·) A14L4 peptide.

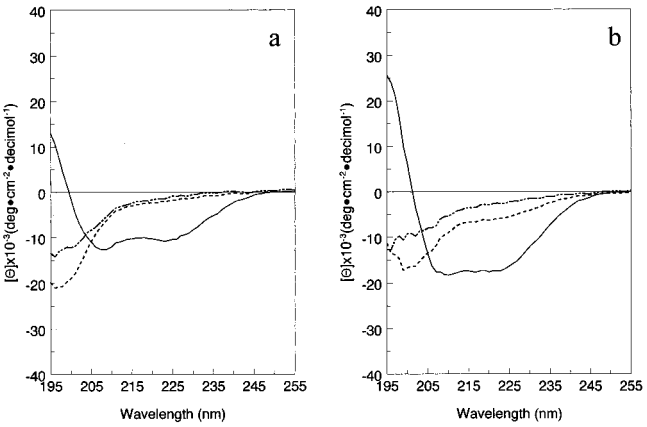

FIGURE 6: Circular dichroism spectra of model membrane-incorporated peptides with sequences derived from the A chain of diphtheria toxin. Samples contained 5 μM peptide in (a) 10-fold diluted Tris-acetate (pH 4.1) or (b) 10-fold diluted Tris-acetate (pH 4.1) with 200 μM 4:1 DOPC/DOPG SUV: (— - - —) A chain residues 168−184, (- - -) A chain residues 76−96, and (—) A chain residues 123−141.

Previous studies showed the CP peptide also exhibits some helix formation in solution at low pH, and an increase in the level of helix formation in the presence of lipid. However, in both the absence and presence of lipid, the CP peptide exhibits significantly less helix formation than the Ala-rich peptides (*26*).

Reversibility of Peptide-Induced Changes in T Domain Conformation. One important question is whether the peptide-induced changes in T domain conformation are reversible. To examine if this is the case, gel filtration chromatography was performed on samples containing the model membrane-inserted T domain to which peptide was added prior to chromatography. Figure 7 shows the elution profiles for samples to which the CP peptide, A16L2 peptide, or no peptide had been added, and Table 3 summarizes shifts in badan fluorescence upon peptide addition and again after chromatography. As shown in Table 3, the blue shift in the fluorescence of badan-labeled residue 356 that is induced by the A16L2 peptide was mostly reversed after chromatography, although the blue shift induced by the CP peptide was not. The difference in A16L2 peptide and CP peptide binding to lipid can explain this difference. The elution profiles in panels a and b of Figure 7 show that the A16L2 peptide largely separates from the vesicle-containing fractions after chromatography, whereas the CP peptide remains in the vesicle fractions.[6] This difference in behavior reflects the relative difference in the strength of the binding of these peptides to lipid,[7] as shown by the data in Figures 2 and 3, and explains the difference in reversibility. The loss of almost all of the A16L2 peptide in the vesicle-containing fractions during chromatography must be sufficient to induce dissociation of most of the A16L2 peptide bound to the membrane-inserted T domain. This means that the formation of the deeply inserted conformation can be reversible.

It should be noted that a similar difference in reversibility of the effects of the A16L2 peptide and CP peptide on T domain conformation was found when samples containing lipid, the badan-labeled T domain, and peptide were simply diluted several-fold (not shown).

The chromatographic elution profiles in Figure 7 also show that the peptides did not induce vesicle fusion. The elution profiles show large vesicles in fractions 16−20 and small vesicles in fractions 20−34. The lipid elution profile in the absence of peptide (Figure 7C) was not strongly altered by the presence of either the A16L2 peptide or CP peptide, indicating a lack of peptide-induced fusion. Furthermore, the T domain was largely associated with the SUV-containing fractions in both the presence and absence of peptides. The question of vesicle size is significant because if the T domain was associated with small vesicles before peptide addition and large vesicles after peptide addition, then fusion rather than peptide−T domain interaction could have been responsible for the peptide-induced blue shift in badan fluorescence. The reason for this is that previous experiments have shown that the T domain forms the deeply inserted conformation in large unilamellar vesicles much more easily than it does in small unilamellar vesicles (*18*).[8]

DISCUSSION

Effect of the Details of Peptide Sequence on Interaction with the T Domain. The membrane-inserted T domain has the ability to bind to a variety of partly unfolded proteins (*18*). This is an unusual ability, because it involves the interaction between two hydrophobic proteins immersed in a lipid environment (i.e., the membrane-bound T domain and a membrane-bound protein in a molten globule-like state). This property is particularly interesting because it may be related to the mechanism by which it translocates the A chain across the bilayer (see below).

The basis of the interaction between the T domain and proteins in the molten globule conformation, or whether this

[6] After adjustment for the scale difference for the samples containing the A16L2 peptide in Figure 7 is made, Trp fluorescence indicates some A16L2 peptide remains lipid bound after chromatography.

[7] Since peptides were added in a very large excess over the T domain, their association with vesicles must overwhelmingly reflect binding to lipid rather than to the membrane-bound T domain.

[8] In view of the relatively low peptide concentrations needed to induce the change in T domain conformation (e.g., a half-maximal blue shift at 2 μM CP peptide), and the observation that the A14L4 and A16L2 peptides are equally effective at inducing this conformational change despite having significantly different levels of binding to lipid vesicles, it seems unlikely to us that peptide-induced perturbations of lipid structure are a dominant influence on T domain conformation.

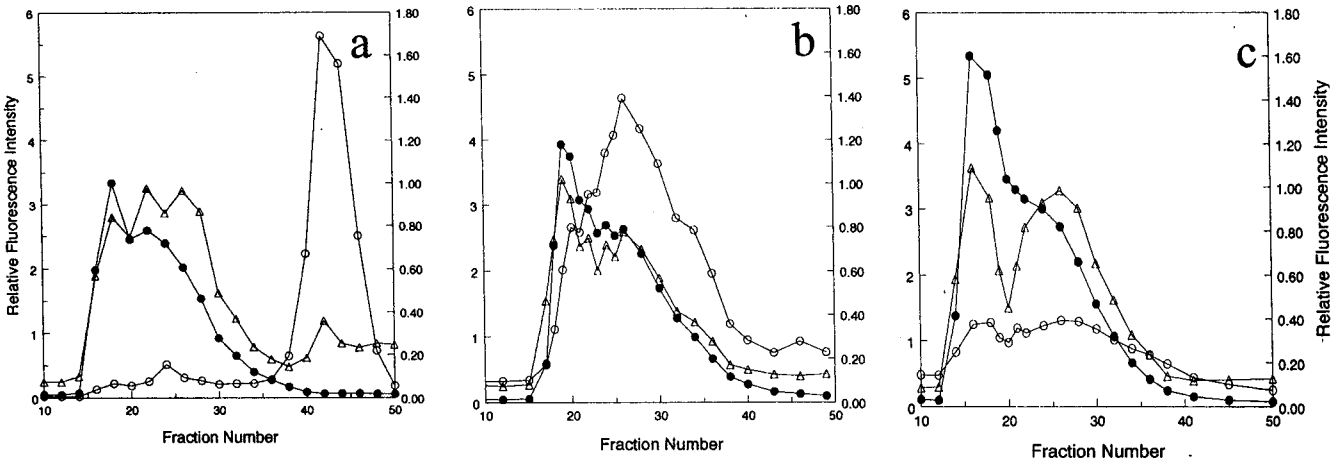

FIGURE 7: Size chromatography of samples containing the model membrane-inserted T domain with and without peptide. Samples contained 1 mM 4:1 DOPC/DOPG vesicles and 7.5 μg/mL badan-labeled A356C T domain to which (a) 50 μM A16L2 peptide, (b) 6 μM CP peptide, or (c) no peptide was added. These samples were chromatographed on a Sepharose 4B-CL column in Tris-acetate (pH 4.1). Right *y*-axis scale: (○) Trp fluorescence and (△) badan fluorescence. Left *y*-axis scale: (●) rhodamine fluorescence. Notice the data for Trp fluorescence in panel a have been multiplied by 0.1 to display it on scale.

Table 3: Badan Wavelength Shifts before and after Chromatography on Sepharose 4B in Samples Containing the T Domain Labeled with Badan at Residue 356 and Inserted into 4:1 DOPC/DOPG Model Membranes[a]

	F_{502}/F_{470} of the badan-labeled T domain		
	none	50 μM A16L2	6 μM CP
before addition of peptide	0.95	0.96	0.98
after addition of peptide	NA	0.75	0.82
after chromatography	1.01 ± 0.04	0.88 ± 0.01	0.81 ± 0.03

[a] The F_{502}/F_{470} values after chromatography are the averages (±standard deviation) of the values in fractions 24, 26, and 28. NA, not applicable.

interaction is even restricted to molten globule-like proteins (i.e., whether unfolded polypeptides in a random coil state would bind to the T domain), is not known. It does seem that, unlike other protein−protein interactions within membranes, tight van der Waals interactions between closely fitting residues are very unlikely to be the driving force of this interaction, because it is not highly specific for particular proteins.

To explore this behavior further, we chose to examine the interaction of a variety of peptides with the membrane-inserted T domain. The results of this study show that the T domain will not interact with every unfolded sequence. In particular, no interaction was found with any sequence that was fully disordered, nor was there any interaction with sequences found within the A chain. Instead, the results suggest that some sort of hydrophobic surface is one factor necessary for allowing polypeptide interaction with the T domain. In addition, the fact the T domain can recognize peptides predominantly composed of polyalanine sequences suggests that a large number of specific interactions between peptide side chains and the T domain are not required for association with the T domain. Nevertheless, hydrophobicity is unlikely to be the only requirement for interaction of amino acid sequences with the T domain. It is noteworthy that the A18L2 peptide and A16L4 peptide interact similarly with the T domain despite having significantly different levels of hydrophobicity, at least as judged by how tightly they bind to lipid vesicles. Furthermore, the CP peptide, which has a complex sequence capable of a variety of interactions, induces the formation of the deeply inserted T domain conformation very effectively. In contrast, the A chain peptide of residues 123−141 was hydrophobic enough to interact with lipids, but did not interact significantly with the T domain.

There could be a role for Coulombic type electrostatic interactions between the A chain and T domain. All of the peptides used in this study were cationic under the experimental (i.e., low pH) conditions that were employed, whereas the segments of the T domain containing the hydrophobic sequences should be anionic at neutral pH, and are likely to remain partly so at endosomal pH (*1*, *33*, *34*). Nevertheless, it is unlikely that electrostatic interactions of this type dominate peptide−T domain interaction, as the (SG)8L2 peptide fails to interact significantly with the T domain, despite having the same number of cationic residues as the other Ala-rich peptides. In addition, the A chain peptides we examined should all be cationic at low pH, but did not interact significantly with the T domain.

In this regard, the strong interaction of the CP peptide with the T domain is intriguing. Unlike the other peptides that were examined, the CP peptide had a large number of Glu residues (seven). This might mean that carboxyl groups, perhaps even if uncharged, do somehow contribute to interaction with the T domain.

Although the peptides that bound the T domain had partially helical structures, it is difficult to make a strong statement about the effect of secondary structure on peptide−T domain interaction. It is possible the peptides we studied have a different secondary structure when bound to the T domain. Unfortunately, the secondary structure of the peptides bound to T domain is very difficult to determine because obtaining a peptide fully complexed with the T domain would require an excess of the T domain. The overwhelming CD signal of the protein would prevent observation of peptide CD. In the native state, the A chain itself has a mix of secondary structures, including several β-strands with some potential to form a transmembrane structure with a hydrophobic face [i.e., alternating hydrophobic and hydrophilic residues ~10 residues in length (*35*)],

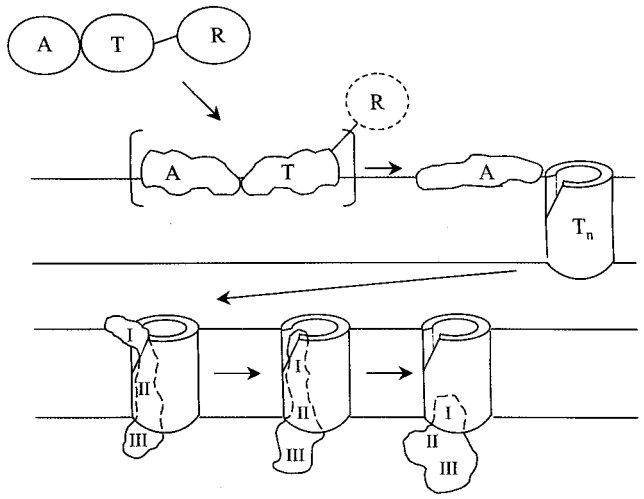

FIGURE 8: Schematic illustration of the chaperone model for translocation. I, II, and III represent sites that interact consecutively with "walls" of the tunnel formed by the T domain. The degree (if any) of oligomerization of the T domain in the transmembrane conformation is undefined.

and no hydrophobic helices. Thus, it is unlikely that the T domain can only bind to helices. Perhaps the membrane-bound T domain can interact with a variety of secondary structural elements.

It is also noteworthy that the intact A chain interacted with the T domain much more strongly than any of the polyalanine peptides. One possible explanation for this is that there are special A chain sequences that strongly bind the T domain, and that these were not among the A chain sequences we chose for detailed study. However, the existence of such special sequences seems unlikely given our previous observation that a variety of molten globule state proteins unrelated to the A chain not only interact with the T domain but also do so significantly more strongly than the A chain (*18*). It seems more likely that the partly unfolded intact A chain forms a more extensive hydrophobic surface than that which can be formed by individual polyalanine peptides. A more extensive hydrophobic surface might allow a number of simultaneous weak interactions, which could multiply together to form a relatively strong interaction between the A chain and T domain.

Chaperone ("Sticky Pore") Model for A Chain Translocation. The chaperone model postulates that during the translocation process the pore-forming T chain acts like a chaperone for a partly unfolded and hydrophobic form of the A chain (*18*). The translocation process could involve a series of transient association steps in which the A chain passes through the membrane with different segments sequentially adhering to the walls of a relatively nonspecific sticky pore formed by the T domain (Figure 8). This would allow translocation of the A chain in a manner that prevents its premature folding, while not requiring that the T domain somehow contain numerous specific binding sites each able to recognize a different part of the A chain sequence. (The possibility that the A chain contacts lipid for some portion of the translocation process is not ruled out by this model.)

The chaperone model is consistent with a number of observations, including (1) at low pH the A chain reversibly unfolds (acquiring a molten globule-like conformation) and becomes hydrophobic (*5*), (2) A chain unfolding is necessary for efficient translocation (*7*, *9*), (3) the membrane-inserted T domain will bind to a number of different proteins as long as they are in the partly unfolded, hydrophobic, molten globule state (*18*), and (4) translocation of a variety of peptide and protein extensions connected to the N-terminal end of the A chain will occur so long as these "passengers" are not fully folded (*31*, *32*). Thus, *one* key prediction of the chaperone model is that the T domain should be able to recognize a variety of amino acid sequences that, like molten globule proteins, have some degree of hydrophobicity and some secondary structure but are unfolded in the sense of having no fixed tertiary structure. The recognition of various medium-length peptides with these properties by the T domain is consistent with this prediction.

CONCLUSION

The mechanism of toxin translocation across membranes remains a complex problem. Although the ability of the T domain to recognize simple, hydrophobic peptides is likely to reflect a property that is important for A chain translocation, and is consistent with the chaperone model, it does not show that the chaperone model is correct. Determining whether the toxin is able to translocate molten globule conformation proteins across membranes in the absence of the A chain may provide a more direct test of the chaperone model.

ACKNOWLEDGMENT

We thank the lab of Y. Peng Loh (National Institutes of Health) for the gift of the CP peptide, Michael Rosconi for purifying and labeling some of the T domain protein used in this study, and Masatoshi Hayashibara for the gift of the purified A chain.

REFERENCES

1. Choe, S., Bennett, M. J., Fuji, G., Curmi, P. M. G., Kantardjieff, K. A., Collier, R. J., and Eisenberg, D. (1992) *Nature 357*, 216−222.
2. Naglich, J. G., Metherall, J. E., Russell, D. W., and Eidels, L. (1992) *Cell 69*, 1051−1061.
3. London, E. (1992) *Biochim. Biophys. Acta 1113*, 25−51.
4. Zhan, H., Choe, S., Huynh, P. A., Finkelstein, A., Eisenberg, D., and Collier, R. J. (1994) *Biochemistry 33*, 11254−11263.
5. Zhao, J.-M., and London, E. (1988) *J. Biol. Chem. 263*, 15369−15377.
6. Montecucco, C., Schiavo, G., and Tomasi, M. (1985) *Biochem. J. 231*, 123−128.
7. Tortorella, D., Sesardic, D., Dawes, C. S., and London, E. (1995) *J. Biol. Chem. 270*, 27446−27452.
8. Jiang, J. X., Chung, L. A., and London, E. (1991) *J. Biol. Chem. 266*, 24003−24010.
9. Falnes, P. O., and Olsnes, S. (1995) *J. Biol. Chem. 270*, 20787−20783.
10. Madshus, I. H., Wiedlocha, A., and Sandvig, K. (1994) *J. Biol. Chem. 269*, 4648−4652.
11. Senzel, L., Gordon, M., Blaustein, R. O., Oh, K. J., Collier, R. J., and Finkelstein, A. (2000) *J. Gen. Physiol. 115*, 421−434.
12. Papini, E., Schiavo, G., Tomasi, M., Colombatti, M., Rappuoli, R., and Montecucco, C. (1987) *Eur. J. Biochem. 169*, 637−644.
13. Kagan, B. L., Finkelstein, A., and Colombini, M. (1981) *Proc. Natl. Acad. Sci. U.S.A. 78*, 4950−4954.
14. Lanzrein, M., Sand, O., and Olsnes, S. (1996) *EMBO J. 15*, 725−734.

15. Eriksen, S., Olsnes, S., Sandvig, K., and Sand, O. (1994) *EMBO J. 13*, 4433−4439.
16. Papini, E., Sandona, D., Rappuoli, R., and Montecucco, C. (1988) *EMBO J. 7*, 3353−3359.
17. Sharpe, J. C., and London, E. (1999) *J. Membr. Biol. 171*, 209−221.
18. Ren, J., Kachel, K., Malenbaum, S. E., Collier, R. J., and London, E. (1999) *Science 284*, 955−957.
19. Lew, S., and London, E. (1997) *Anal. Biochem. 251*, 113−116.
20. Ren, J., Lew, S., Wang, Z., and London, E. (1997) *Biochemistry 36*, 10213−10220.
21. Wang, Y., Malenbaum, S. E., Kachel, K., Zhan, H., Collier, R. J., and London, E. (1997) *J. Biol. Chem. 272*, 25091−25098.
22. Bolen, E. J., and Holloway, P. W. (1990) *Biochemistry 29*, 9638−9643.
23. Sreerama, N., Venyaminov, S. Y., and Woody, R. W. (1999) *Protein Sci. 8*, 370−380.
24. Kachel, K., Ren, J., Collier, R. J., and London, E. (1998) *J. Biol. Chem. 273*, 22950−22956.
25. Weber, G., and Farris, F. J. (1979) *Biochemistry 18*, 3075−3078.
26. Dhanvantari, S., Arnaoutova, I., Snell, C. R., Steinbach, P. J., Hammond, K., Caputo, G. A., London, E., and Loh, Y. P. (2002) *Biochemistry 41*, 52−60.
27. McKnight, C. J., Rafalski, M., and Gierasch, L. M. (1991) *Biochemistry 30*, 6241−6246.
28. Volgino, L., Simon, S. A., and McIntosh, T. J. (1999) *Biochemistry 38*, 7509−7516.
29. Eftink, M. R., and Ghiron, C. A. (1976) *Biochemistry 15*, 672−680.
30. Kachel, K., Asuncion-Punzalan, E., and London, E. (1995) *Biochemistry 34*, 15475−15479.
31. Madshus, I. H., Olsnes, S., and Stenmark, H. (1992) *Infect. Immun. 60*, 3296−3302.
32. Wiedlocha, A., Madshus, I. H., Mach, H., Middlaugh, C. R., and Olsnes, S. (1992) *EMBO J. 11*, 4835−4842.
33. London, E., Blewitt, M. G., Chattopadhyay, A., Chung, L. A., and Zhao, J.-M. (1986) in *Protein Engineering: Applications in Science, Medicine and Industry* (Inouye, M., and Sarma, R., Eds.) pp 95−110, Academic Press, New York.
34. Ren, J., Collier, R. J., and London, E. (1999) *Biochemistry 38*, 976−984.
35. London, E. (1992) *Mol. Microbiol. 6*, 3277−3282.
36. Kachel, K., Asuncion-Punzalan, E., and London, E. (1998) *Biochim. Biophys. Acta 1374*, 63−76.

BI011163I